CONTRACT NUMBER: N00014-77-C-00457
MODIFICATION NO: P00001

WF 1 385575 4/6/78 L+L

R&D STATUS REPORT

(12) 33

ARPA ORDER NO.: #2840 PROGRAM CODE NO.: N63375

CONTRACTOR: Stanford University (9) Research and development status rept. 1 Jan-1 Mar 78,

CONTRACT NO.: (15) N00014-77-C-0457, CONTRACT AMOUNT: $52,035.00

ARPA Order-2840

EFFECTIVE DATE OF CONTRACT: November 16, 1977

EXPIRATION DATE OF CONTRACT: November 15, 1978

PRINCIPAL INVESTIGATOR: Professor (10) Richard N. Zare

TELEPHONE NO.: 415/497-3062

SHORT TITLE OF WORK: (6) Research on Metal Halide Laser Systems.

REPORTING PERIOD: January 1, 1978 - March 1, 1978

(11) 19 Jul 78

During this period we investigated the production of excited metal atoms by the photodissociation of volatile metal--encapsulated compounds. Specifically, we studied $FE(CO)_5$, $Fe(CO)_3$, $CH_2CHCHCH_2$, 1,1'dimethyl, ferrocene, $Ni(CO)_4$, $Zn(CH_3)_2$, $Mn(CO)_5Cl$ and $Mn(CO)_6$. In all cases atomic emission is observed when a few torr of the parent compound is irradiated by the 2458Å output of a KrF laser (15mJ/pulse). Most of this grant period was devoted to the fabrication of the KrF laser. This device is presently operational and plans are underway to modify it so that it will also operate as a ArF laser (1930Å output).

Future plans will involve a comparison of the atomic emission to that excited by electron impact. For this purpose, we have arranged to use the Febetron facility of SRI International. The population of different spin manifolds appears to differ

352362

STANFORD UNIVERSITY
STANFORD, CALIFORNIA 94305

DEPARTMENT OF CHEMISTRY

July 19, 1978

Dr. Al Wood
ONR Branch Office
495 Summer Street
Boston, MA 02210

Ref: Contract No. N00014-77-C-0457

Dear Dr. Wood:

At your request, I am sending you a one page letter summarizing our work from December 15, 1977 through the present.

As a natural outgrowth of our metal halide laser research program, we have begun exploring the possibility of developing a new class of lasers based on the decomposition of volatile metal carriers (metal-encapsulated compounds) such as iron pentacarbonyl, $Fe(CO)_5$, thalium trimethyl $Tl(CH_3)_3$, lead tetramethyl $Pb(CH_4)_4$ and zinc dimethyl Zn $(CH_3)_2$. Our initial experiments involve the use of a home-built rare gas halide laser, either KrF at 249 nm or ArF at 193 nm, to photolyze these compounds.

We find that this technique provides a general method for producing excited metal atoms. In all cases we observe that the excited state atom production (1) involves the absorption of more than one photon, (2) proceeds in the absence of collision, and (3) populates only certain specific excited state levels. Moreover, the addition of buffer gas (e.g. 300 torr He or Ar) causes an enhancement in the emission intensity as well as the appearance of new lines and in one case what appears to be molecular emission. In the coming months we will be pursuing the question of whether such systems can be made to lase by optical pumping. We have also initiated experiments at SRI International to discover how the emission characteristics change when one uses e-beam pumping.

Finally, I will close by telling you about the contract finances. Of the total funds ($52,035), on the start of June, 1978, we had a balance of $1,635 which was not obligated. Consequently, I expect to expend all funds on or (more likely!) before the contract termination date of December 15, 1978.

Sincerely yours,

Richard N. Zare

Richard N. Zare
Professor of Chemistry

cc: Distribution List

RNZ:af

(12)

sharply from that seen in arc spectra. We are interested in this phenomona not only as a way to understand the mechanism of polyatomic metal--organic dissociation but also to evaluate its possible use as a laser medium.

The fiscal status reflects the fact that we have committed the capital equipment funds, although most items have not yet been received.

Salary and Wages	$ 712.50
Staff Benefits	135.38
Expendables	3,707.04*
Capital Equipment	-0-
Travel	-0-
Total Direct Costs	4,554.92
Total Indirect Costs	2,641.85
Total Expenditures	7,196.77

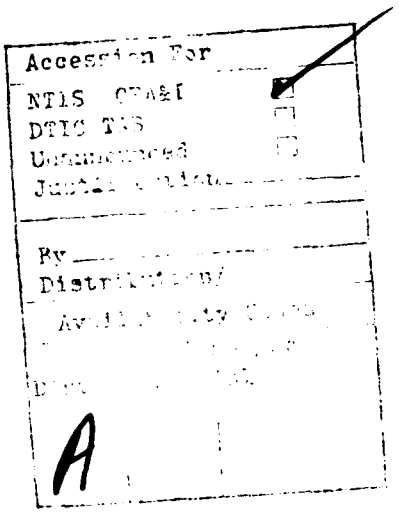

Commitments:

Salary and Wages	$ 2,523.50
Staff Benefits	479.47
Travel	-0-
Expendables	137.00
Total Commitments	3,139.97
Total Expenditures and Commitments to date	$ 10,336.74

Funds required to complete work: $24,663.00

*To date $3,069.96 of expendables reflects costs for fabrication of capital equipment.

wjc 395-575
LTF
1/3/78

ANNUAL REPORT

ARPA Order Number:	2840, Amend. #6
Program Code Number:	421
Contractor:	Stanford University
Start Date of Contract:	June 15, 1977
Expiration Date of Contract:	November 15, 1977
Amount of Contract:	$17,035
Contract Number:	N00014-77-C-0457
Principal Investigator:	Richard N. Zare Professor of Chemistry
Scientific Officer:	Dr. Robert Behringer Office of Naval Research Pasadena Branch Office 1030 East Green St. Pasadena, CA 91106
Short Title of Work:	"Absolute Photon Yields"
Sponsored by:	Advanced Research Projects Agency ARPA Order No. 2840/6

File contracts

Disclaimer:

The views and conclusions contained in this document are those of the author and should not be interpreted as necessarily representing the official policies, either expressed or implied, of the Advanced Research Projects Agency or the U.S. Government.

INTRODUCTION

Description/Specifications:

"The Contractor shall establish a standard procedure for the measurement of absolute photon yields for chemiluminescent reactions over the pressure range from 0.1 mtorr to a few torr of inert gas. Toward this end the Contractor shall measure the photon flux, the metal flux, the oxidant flux, the chemiluminescence cross section and the total cross section for the reaction of Sm with nitrous oxide."

So began this study on December 3, 1975 in the Department of Chemistry, Columbia University. Since then, the above objectives have been fulfilled (see attached publications) and the principal investigator has moved to the Department of Chemistry, Stanford University, this last summer. The following is a technical report of our activities and accomplishments during the 5-month period at Stanford under contract N00014-77-C-0457.

Our major activity during the period of the grant was to re-establish the operation of our laboratory, particularly, our capability to run high-temperature chemical reactions in a beam-gas configuration. I am pleased to report that by early September this facility became fully operational.

Not everything survived the move undamaged. This required repairs, especially to our laser systems. These were completed in late October.

Of the $17,000 budgeted for this research program, approximately $7,000 are indirect costs, leaving a grand sum of $10,000 for direct research costs. This amount was roughly divided equally between salaries and expendable supplies, the latter being predominately costs incurred in repair and in setup charges.

Toward the end of this contract, preliminary experiments were begun on the mercury halides. Although such work is not in the contract description/specification, I was instructed at the May, 1977, Contractors' Meeting by Colonel G. Canavan of DARPA that there was no further interest in photon yield measurements. Consequently, our work has been redirected toward metal halide laser systems. Preliminary results show that

$$Hg(^3P_1) + X_2 \rightarrow HgX^* + X$$

where $X_2 = C\ell_2$, Br and I_2. A proposal has been submitted to DARPA requesting funding to continue these studies, since they bear on the construction of electric discharge metal halide lasers.

LIST OF PUBLICATIONS

C. R. Dickson, S. M. George, and R. N. Zare, "Determination of Absolute Photon Yields Under Single-Collision Conditions" Journal of Chemical Physics 67, 1024 (1977).

C. R. Dickson and R. N. Zare, "Spectroscopic Study of Pb + F_2 Chemiluminescence" Optica Pura y Aplicada (accepted for publication).

395-575

Determination of absolute photon yields under single-collision conditions

C. R. Dickson,[a] S. M. George,[b] and R. N. Zare[c]

Department of Chemistry, Columbia University, New York, New York 10027
(Received 27 December 1976)

The experimental procedure is presented to measure the absolute photon yield, the percentage probability of emitting a visible photon per reactant molecule consumed, for chemiluminescent reactions under single-collision conditions. Using a well-defined metal beam directed into a scattering gas at submillitorr pressures, this procedure is applied to the reactions $Sm+N_2O$, $Sm+F_2$, $Ba+N_2O$, and $Ba+NO_2$ to obtain the photon yields in the 350–800 nm range of 0.39%, 11.8%, 2.4%, and 0.18%, respectively, where the estimated uncertainty is about 50%. The absolute photon yields for each of these reactions initially increases with scattering gas pressure, demonstrating that secondary collisions "feed" radiating states from dark, reservoir states. It is suggested that other relative photon yields can be put on an absolute basis by comparison with the $Sm+N_2O$ chemiluminescent reaction.

I. INTRODUCTION

The possibility of a chemically pumped electronic-transition laser system has recently stimulated the measurement of absolute photon yields for several chemiluminescent reactions.[1-6] Some of these reactions are reported to have high photon yields, such as $Sm+F_2$ (~60%),[3] $Sm+N_2O$ (~35%),[3] and $Ba+N_2O$ (~20%).[3,6] All of these measurements were performed at pressures of several torr of argon and the fraction of electronic excitation appearing initially in the reaction products is obscured by the presence of many collisions. Thus, there is considerable interest in photon yield measurements in the submillitorr pressure range, because they provide information about the primary excitation process in a chemiluminescent reaction. We present here absolute photon yields for the reactions $Sm+N_2O$, $Sm+F_2$, $Ba+N_2O$, and $Ba+NO_2$ using a beam-gas arrangement at oxidant pressures of $\sim 10^{-4}$ torr.

Since absolute photon yields have not been determined in the submillitorr pressure range previously, our procedure will be presented in some detail. In particular, the following quantities are measured: the photon flux, the metal flux, the oxidant flux, and the chemiluminescent cross section and the total cross section for the reaction. The photon yield is defined to be the percentage number of photons emitted per oxidant molecule or metal atom consumed. For the beam-gas arrangement this is found from the ratio of the chemiluminescent cross section to the total reaction cross section.

We propose that the reaction of Sm with N_2O can be used as a reference reaction for beam-gas chemiluminescence for several reasons. This reaction appears to be bright under beam conditions as well as in the presence of argon. The spectrum of SmO resulting from this reaction (See Fig. 1) has little structure at low resolution (~5 Å), and the chemiluminescence occurs over a wide range of wavelengths (450–750 nm). Samarium is relatively cheap, undergoes far less oxidation in air than barium, and produces beams of high flux at temperatures easily achieved in most laboratories (1000–1200 °K). A well characterized reaction such as $Sm+N_2O$ now provides a basis for calibration in other laboratories as well as in our own.

II. EXPERIMENTAL

A. Beam apparatus

The beam apparatus LABSTAR, which has been described previously,[7] is used to produce the chemiluminescent reactions. It consists of two differentially pumped chambers, the lower of which is a water-cooled Astro oven containing a cylindrical graphite heater and oven surrounded by three concentric tantalum heat shields (Fig. 2). The metal is heated until the vapor pressure reaches 0.01 to 0.1 torr. The effusive beam of metal enters the upper scattering chamber where it reacts with the oxidant molecules typically at pressures of 10^{-5} to 10^{-4} torr to produce chemiluminescence.

B. Photon flux

The approach often taken is to calibrate an entire optical-detection system (spectrometer, lens, etc.) on an absolute basis to determine the photon flux for a chemiluminescent reaction. This requires that one correct for the change in geometry when the standard lamp is

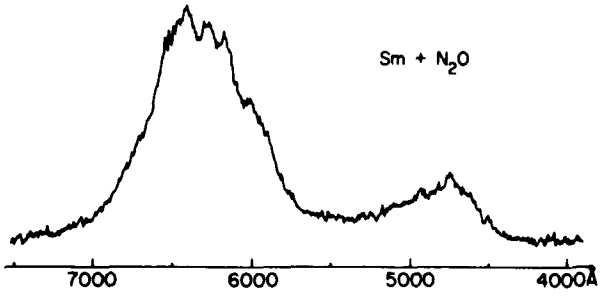

FIG. 1. Beam-gas chemiluminescent reaction of $Sm+N_2O$ taken at a scan rate of 500 Å/min and at a resolution of 5 Å.

[a] Present address: Materials Research Center, Allied Chemical, P. O. Box 1021R, Morristown, NJ 07960.
[b] Present address: Department of Chemistry, Yale University, New Haven, CT 06520.
[c] Present address: Department of Chemistry, Stanford University, Stanford, CA 94305.

TABLE I. Correction factors for chemiluminescent spectra.

λ(Å)	Standard lamp photon flux[a]	Relative photon flux[b]	Relative signal from optical-detection system[c]	Correction factor[d]
3000	0.00409	0.00124	0.001	1.000
3500	0.0288	0.00713	0.049	0.146
4000	0.0891	0.0221	0.202	0.109
4500	0.227	0.0562	0.475	0.118
5000	0.460	0.114	0.764	0.149
5500	0.773	0.191	0.973	0.196
6000	1.163	0.288	0.980	0.294
6500	1.601	0.396	0.881	0.449
7000	2.051	0.508	0.704	0.722
7500	2.515	0.623	0.445	1.400
8000	2.908	0.720	0.217	3.318
9000	3.557	0.880	0.016	55.
10000	4.040	1.000	0.008	125.

[a]photons sec^{-1} cm^{-2} nm^{-1} × 10^{12}.
[b]See Fig. 3(c).
[c]See Fig. 3(a).
[d]See Fig. 3(b).

placed at the position of the reaction zone. To avoid this difficulty, we have chosen to calibrate the optical-detection system that generates the spectra on a relative basis. We found that a relative calibration is reproducible to better than 1% under a variety of conditions (various spectrometer slit widths, with and without a lens in place, etc.). The results of the relative calibration of the optical-detection system used in our measurements are given in Table I. Figure 3 shows how the correction factors listed in Table I are generated. A scan of the standard lamp output is made with the spectrometer [Fig. 3(a)]. Figure 3(b) is a plot of the correction factors by which the standard lamp output [Fig. 3(a)] is multiplied to obtain the actual photon flux output of the standard lamp [Fig. 3(c)].

The spectrometer and optics (including the standard lamp) is aligned by means of a helium–neon laser. The common belief that uncalibrated lamps have the same absolute spectral output within 15% of that for a calibrated lamp is not correct. To obtain results better than 10% with a standard lamp (Optronic Laboratories model 245C) the current must be regulated to better than 0.1%

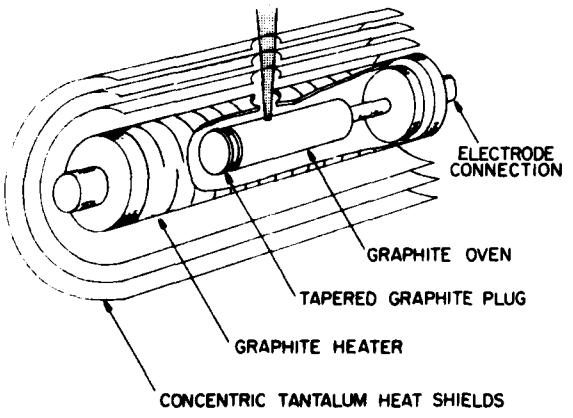

FIG. 2. Metal atom source, designed by R. C. Oldenborg.[7] A few hundred amperes are passed through a graphite cylinder, held between two water-cooled copper bussbars. The graphite heater has slots cut on its body to increase the resistance. Inside the heater and supported from one end is a graphite crucible containing the metal sample.

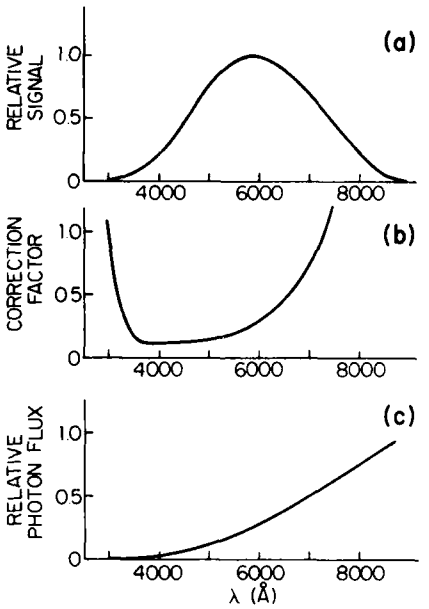

FIG. 3. (a) The spectrum of the standard lamp output,[8] which is multiplied by the correction factor (b) to obtain (c) the relative photon flux of the standard lamp. In practice, (a) and (c) are known, while (b) is derived.

and the actual current measurement must be made better than 1%. The current may be measured by monitoring the voltage drop across a precision resistor with a digital voltmeter. Alternatively, the power supply (Optronic Laboratories model 65) may be used. Since this supply maintains the required 6.50 A to better than 0.1%, we have chosen the use of the power supply to ensure the best calibration. It is important that the lamp orientation and the polarity of the electrical connections to the lamp are made in the manner specified by the manufacturer if reproducible results are desired.

To obtain an absolute calibration of the spectra corrected on a relative basis a photomultiplier tube behind a slit of known area views the chemiluminescence through three different interference filters having a narrow bandwidth (< 30 Å). This optical-detection system (see Fig. 4) is calibrated on an absolute basis with the standard tungsten–iodine lamp. The calibrated output is listed in Table II for each interference filter. Thus, the need to

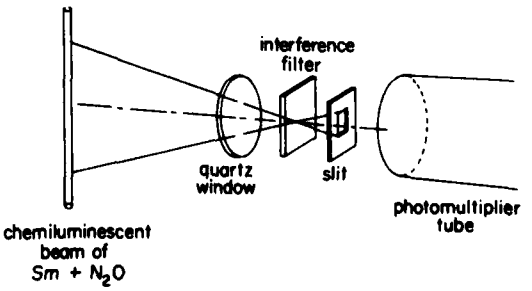

FIG. 4. Photon flux measurement apparatus. The distance from the beam to the slit is about 10.5 cm. The slit is a rectangular aperature, 0.3 cm high and 1.0 cm long.

TABLE II. Phototube and interference filter calibration.

λ(Å)	FWHM(Å)	Phototube calibration[a]
6328.0	34	3.99×10^{14}
5262.5	17.5	8.39×10^{14}
4418.0	33	1.97×10^{14}

[a]photons sec^{-1} nm^{-1} cm^{-2} A^{-1}.

calibrate a spectrometer and lens arrangement on an absolute basis is entirely eliminated. While only one interference filter is necessary to provide an absolute calibration at all wavelengths, three such filters provide cross checks.

The Sm beam enters the scattering chamber through a 4.1 mm diameter hole, and the chemiluminescence appears as a very narrow, cylindrical beam of light. The geometry of the beam is not diffuse for the reaction of $Sm + N_2O$ because the radiative lifetime of SmO is 83 ± 2 nsec.[9]

Let the chemiluminescent emission per unit volume be denoted by E. Then the photon flux (F_D) at the detector is given by

$$F_D = A_D E V_{obs}/4\pi r^2 \quad , \tag{1}$$

where A_D is the aperture area (0.3×1 cm) and V_{obs} is the volume of chemiluminescence defined by the detector field of view through the aperture. The volume of chemiluminescence (V_{obs}) actually observed was determined in two ways. A mask was gradually lowered into the field of view until a decrease in the chemiluminescent intensity was measured. From this observation we derive V_{obs} from a knowledge of the beam cross section. A second determination was made by surrounding the beam by a tube (~2 cm diam.) having its inside blackened. This tube had a 0.4×1 cm aperture which defined the reaction zone visible to the photomultiplier. The ratio of the chemiluminescent intensities without and with this additional slit should be the ratio V_{obs} to the known value of V_{obs}. The two V_{obs} determinations agreed within 8%. A more complete discussion is given in the Appendix.

To determine the number of photons emitted per second from this volume the chemiluminescent spectrum is corrected on a relative basis using the correction factors of Table I. The area under the chemiluminescent spectrum is proportional to the number of photons emitted per second. The absolute number of photons emitted per second is obtained by observing the chemiluminescence through an interference filter whose output is calibrated on an absolute basis (Table II). The total number of photons emitted per second in all directions is then found from Eq. (1). The spectrum range covered is 350–800 nm.

C. Metal flux

Because the "sticking coefficient" is not unity for most metals, quartz microbalance techniques and other thin film thickness monitors only measure the amount of metal actually deposited on the sensor and *not* necessarily the true metal beam flux. Consequently, we chose to collect the metal beam using a thin, hollow, glass sphere having an entrance port slightly larger then the beam diameter (see Fig. 5). Since little metal can escape, we expect the results to be reliable. The amount of metal deposited over a given time period is then determined by weighing the collection vessel before and after deposition. In the case of barium the metal was allowed to convert completely to the oxide so that the best determination of the original amount of metal could be made. Five determinations were made of the Sm flux by collecting the metal over a 3 h period. The average weight was 0.0106 ± 0.0021 g. This corresponds to a Sm flux of 4.53×10^{15} atoms/cm^2 sec at the glass sphere 11 cm distant from the oven. Similarly, the barium flux was found to be 1.77×10^{16} atoms/cm^2 sec under the same conditions.

D. Oxidant flux

Pressure measurements are made with a corrosion-resistant capacitance manometer (Datametrics model 573A-10T-4A1-H5). Depending on the particular gas, the pressure read by an ionization gauge can be in error by a factor of 2 or 3 in the pressure range of 10^{-4} torr. Because of the reactivity of the various oxidant gases used, we found it impossible to calibrate an ion gauge against the capacitance manometer. The input port of the capacitance manometer (3/8 in. stainless steel tube approximately 6 in. long) was less than 1/4 in. away from the reaction zone viewed by the photomultiplier when the photon flux was being measured. Efforts were made to eliminate any adsorbed water this tube by heating it with a heat gun while the chamber was being evacuated. When the tube cooled sufficiently it could be accurately zeroed and remained reasonably stable over a few minutes before the zero would have to be readjusted slightly.

The reliability of capacitance manometer measurements has been checked by Loriot and Moran[10] against the absolute pressure as measured by a McCleod gauge in the submillitorr pressure range. They find that the difference is ~0.6% over the pressure range 2×10^{-4} to 5×10^{-6} torr. Thus, we feel that the use of a capacitance manometer gives a trustworthy determination of the oxidant pressure.

E. Cross section measurements

At low pressures (10^{-5} to 10^{-4} torr) the chemiluminescence intensity obeys a $p\exp(-\alpha p)$ relationship, where p is the oxidant pressure.[7] The linear term in p describes

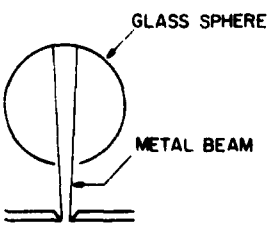

FIG. 5. Metal flux determination using a thin, hollow, glass sphere. In order to obtain a weighable sample the orifice of the entrance port to the scattering chamber is enlarged. While the number of metal atoms/sec that are collected increases, the flux (number of metal atoms/cm^2 sec) is not altered by the small change made.

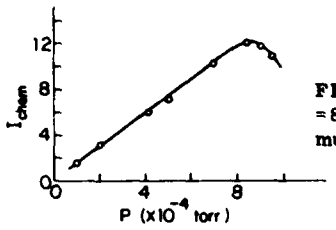

FIG. 6. Determination of σ_{tot} = 82 Å^2 from the pressure maximum for Sm + N_2O.

the formation of excited state molecules and the exponential term $\exp(-\alpha p)$ describes the attenuation of the metal beam by the oxidant. The attenuation parameter α in torr^{-1} is related to the total phenomenological cross section for metal atom removal σ_{tot} in Å^2 by

$$\alpha = 1.33\times10^{-13}\,\frac{l\sigma_{tot}}{kT}\ , \tag{3}$$

where l is the beam path length (cm) in the reaction chamber from the port of entry to the reaction zone viewed by the spectrometer, k is the Boltzmann constant (erg °K^{-1} molecule^{-1}), and T is the absolute temperature. The constant 1.33×10^{-13} has units of dyne torr^{-1} Å^{-2}. The attenuation parameter can be determined in two independent ways:

(1) by studying the chemiluminescence intensity vs oxidant pressure for constant l;

(2) by studying the chemiluminescence intensity vs l for a constant oxidant pressure.

The first method determines α from the pressure maximum

$$\alpha = 1/P_{max}\ , \tag{4}$$

from which σ_{tot} may be found using Eq. (3). A typical plot for the Sm + N_2O reaction is given in Fig. 6. Although the chemiluminescent intensity appears linear with oxidant pressure for low pressures, the falloff is more rapid than expected. Consequently, the use of Eq. (4) to determine α is only a rough estimate. The second method plots $\ln I$ vs l (see Fig. 7); the slope of this plot is given by

$$\frac{d(\ln I)}{dl} = -1.33\times10^{-13}\left(\frac{P}{kT}\right)\sigma_{tot}\ , \tag{5}$$

from which σ_{tot} can be directly determined. The latter method is preferable since higher oxidant pressures are avoided.

TABLE III. Total phenomenological cross sections.

Reaction	σ_{tot}(Å^2) I_{chem} vs length[a]	I_{chem} vs pressure[b]
Sm + N_2O	89 ± 6	82
Sm + F_2	99 ± 8	95
Ba + NO_2	···	122
Ba + N_2O	82 ± 6	92

[a]See Eq. (5). [b]See Eq. (4).

TABLE IV. Absolute photon yields (%) as a function of pressure.[a]

P (10^{-4} torr)	Sm + N_2O	Sm + F_2	Ba + N_2O	Ba + NO_2
0.6	0.32 ± 0.13	···	···	···
1.0	0.47 ± 0.15	···	2.25 ± 0.17	0.19
1.2	0.39 ± 0.15	···	···	0.18
1.5	···	11.8 ± 0.9	···	···
1.8	0.43 ± 0.17	···	···	···
2.0	0.60 ± 0.17	···	2.42 ± 0.58	···
2.1	···	···	···	0.17
3.0	···	10.9 ± 0.6	2.59 ± 0.39	···
3.2	···	12.8 ± 1.1	···	···
4.0	0.66 ± 0.09	···	2.33 ± 0.81	···
4.4	···	12.0 ± 0.9	···	···
5.0	0.90 ± 0.24	···	3.42 ± 0.90	···
6.0	···	···	2.91 ± 0.73	···
6.5	···	13.5 ± 0.6	···	···
6.7	···	···	···	0.20
7.0	···	···	3.70 ± 0.92	···
7.3	···	15.0 ± 0.9	···	···
7.5	···	···	3.62 ± 0.96	···
8.5	1.86 ± 0.79	···	···	···

[a]Errors are one standard deviation (σ).

The total phenomenological cross sections for the Sm + N_2O, Sm + F_2, Ba + NO_2, and Ba + N_2O reactions are given in Table III. Equation (5) is used except for Ba + NO_2, and the errors listed represent the maximum variation for five measurements at different pressures.

F. Photon yields

The chemiluminescence intensity (photons sec^{-1}) for the Sm + N_2O reaction is given by

$$I_{chem} = k[M][OX]V_{obs} \tag{6}$$

under single-collision conditions, where V_{obs} is the observed reaction volume (cm^3), k is the rate constant (cm^3 sec^{-1}), and [M] and [OX] are concentrations (number per cm^3). The chemiluminescence cross section σ_{chem} is then determined from the relation

$$I_{chem} = \sigma_{chem}\bar{v}[M][OX]V_{obs}\ , \tag{7}$$

where $\bar{v}$ is the average relative velocity of the metal atoms. Since the initial metal beam flux $[M_0]$ will be attenuated by a factor $e^{-\alpha p}$, this correction is included in estimating [M] in the reaction zone. Thus, the chemiluminescence cross section is given by

$$\sigma_{chem} = \frac{I_{chem}}{(\bar{v}[M_0]e^{-\alpha p})([OX]V_{obs})}\ . \tag{8}$$

In Eq. (8) the first factor in the denominator is the metal

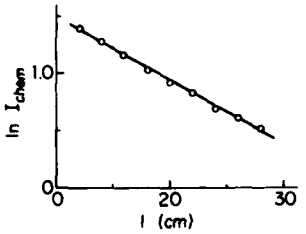

FIG. 7. Plot of the logarithm of the chemiluminescent intensity vs path length for the reaction Sm + N_2O. The data presented give a determination of σ_{tot} = 91 Å^2, which was included in the average reported in Table III.

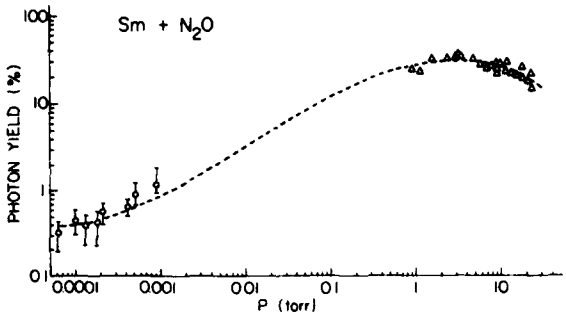

FIG. 8. Absolute photon yields as a function of pressure for the $Sm + N_2O$ reaction: (○) this work; and (△) Ref. 3. The dashed line is drawn to connect smoothly the low and high pressure data; no model is implied.

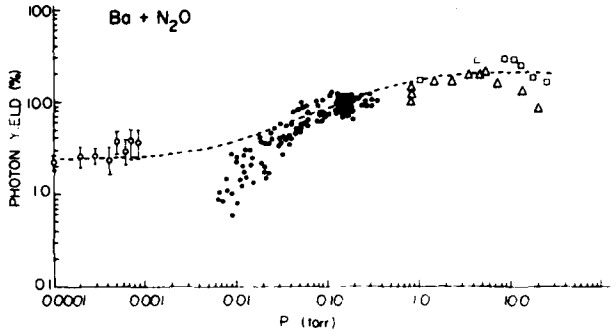

FIG. 10. Absolute photon yields as a function of pressure for the $Ba + N_2O$ reaction: (○) this work; (●) Ref. 11; (△) Ref. 3; and (□) Ref. 6. The dashed line is drawn to connect smoothly the low and high pressure data; no model is implied.

flux (atoms $cm^{-2} sec^{-1}$) in the reaction zone and the second factor is the number of oxidizer molecules in the reaction zone. With I_{chem} in units of photons sec^{-1} the dimensions of σ_{chem} are cm^2. The photon yield in percent is taken to be the ratio of the chemiluminescence cross section to the total cross section

$$\Phi = \frac{\sigma_{chem}}{\sigma_{tot}} \times 100 \quad . \tag{9}$$

Since σ_{tot} includes wide-angle nonreactive scattering processes (e.g., inelastic collisions), Φ is actually a lower bound. However, when the reactive cross section is large, such as in these cases, σ_{tot} is expected to be a good approximation to the total reactive cross section.

III. RESULTS

The photon yields for the reactions $Sm + N_2O$, $Sm + F_2$, $Ba + N_2O$, and $Ba + NO_2$ were determined at various pressures. Often several measurements were made at each pressure and the results, given in Table IV, represent average values. Figures 8–12 show the actual spread in the data for each of the above reactions. The dotted lines connect the absolute photon yields obtained at pressures of several torr argon to the average values in the submillitorr region.

Palmer and co-workers[5,11] have measured photon yields in the 0.01–0.1 torr pressure regime for the $Ba + N_2O$ and $Ba + NO_2$ reactions. Our measurements provide a low pressure intercept that connects to their data very well. While no measurements exist in the 0.01–0.1 torr pressure range for the $Sm + N_2O$ and $Sm + F_2$ reactions, the dotted line should predict the photon yields where they have not been measured. The intercepts provide data that may help to model the high-pressure reaction kinetics for these systems.

The estimated uncertainties in the absolute photon yields are ~50%, where the estimated uncertainty for σ_{tot} is ~10%, I_{chem} is 10%, [M] is ~20%, and [OX] is ~10%. The most serious error is associated with the metal flux determinations. For the reaction $Sm + N_2O$ at a pressure of 8.5×10^{-4} torr the photon yield was measured 10 times giving $\Phi = 1.86 \pm 0.79$, where the error represents one standard deviation. This error is a 43% uncertainty, but some standard deviations for the $Sm + N_2O$ and $Ba + N_2O$ reactions at other pressures were 10%–20% of the average value. The 50% uncertainty represents an estimate of all errors, statistical and systematic. As can be seen from Table IV the scatter of the measurements is much smaller.

We previously reported a preliminary photon yield of 0.3% for the reaction $Sm + N_2O$ at a pressure of 4×10^{-4} torr.[12] The value at this same pressure given in Table IV is 0.66%. However, the preliminary value did provide a reasonable order of magnitude estimate.

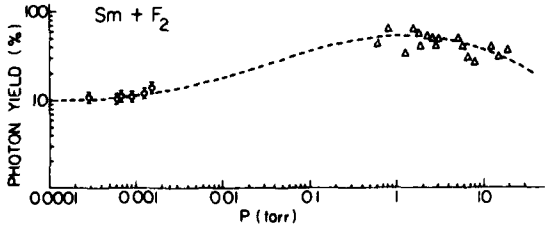

FIG. 9. Absolute photon yields as a function of pressure for the $Sm + F_2$ reaction: (○) this work; and (△) Ref. 3. The dashed line is drawn to connect smoothly the low and high pressure data; no model is implied.

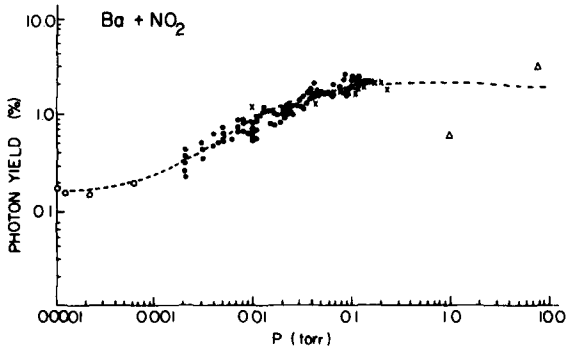

FIG. 11. Absolute photon yields as a function of pressure for the $Ba + NO_2$ reaction: (○) this work; (●) and (×) Ref. 11; and (△) Ref. 6. The dashed line is drawn to connect smoothly the low and high pressure data; no model is implied.

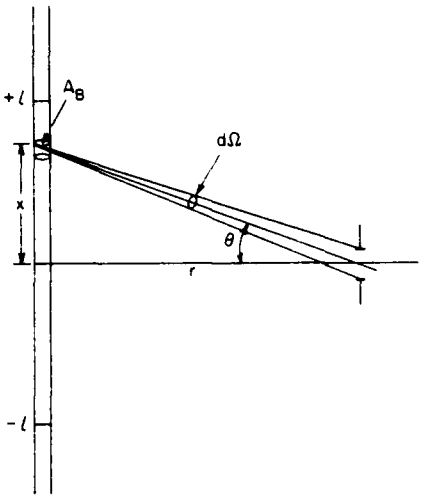

FIG. 12. Geometry for describing the measurement of flux from a finite cylindrical light source.

Yokozeki and Menzinger[13] recently measured *relative* photon yields for several Sm and Yb reactions in the 5×10^{-6}–5×10^{-3} torr range, also using a beam-gas arrangement. They found at $\leq 1\times10^{-4}$ torr that the ratio of the photon yield for the Sm + N_2O reaction to that of the Sm + F_2 reaction is 0.13. This should be compared with our photon yield ratio of 0.036. The large discrepancy arises from the difference between the total reactive cross sections used in these two studies. Because we have two independent measurements on σ_{tot}, we believe our values are to be preferred. A similar disagreement occurs for the reaction of Ba + N_2O under beam conditions. Menzinger[14] finds a total phenomenological cross section of about 30 Å^2. While this agrees with previous work,[7] it disagrees with the present value of 82 Å^2.

One remarkable result of this study is that the absolute photon yield for the Sm + F_2 reaction is ~12% under single-collision conditions. Our previous estimate was only ~1% because of errors associated with the measurements of the F_2 pressure and the determination of V_{obs}. The high photon yield for the Sm + F_2 reaction is very interesting because it suggests that there may be other chemical reactions with an appreciable probability for producing electronically excited products in the initial reaction step.

ACKNOWLEDGMENTS

We thank D. J. Eckstrom for critically reading an earlier draft of this paper and for helping us to calculate the photon flux. We are also grateful to H. B. Palmer and M. Menzinger for providing us with unpublished data. This research was supported by the Advanced Research Projects Agency of the Department of Defense, monitored by the Office of Naval Research under contract N00014-76-C-0466, and by the Air Force Office of Scientific Research under contract AFOSR-73-2551.

APPENDIX: PHOTON FLUX FROM A CYLINDRICAL CHEMILUMINESCENT BEAM

The following considerations are due to D. J. Eckstrom, who provided us with the calculations of the photon flux from a cylindrical light source of variable extent: The chemiluminescent beam is assumed to have a cross section A_B of uniform emission. The aperture through which the emission is viewed is at a distance r and has an area A_D. The detector is capable of viewing the chemiluminescence over a distance $+l$ to $-l$ as shown in Fig. 12. If the emission per unit volume is

$$E(x)=\sigma_{chem}\bar{v}\,[M_0 e^{-\sigma_{tot}Nx}]\,[OX]\quad , \tag{A1}$$

where N is the number of oxidant molecules per unit volume, then the photon flux at the detector is

$$F_D=\int_{-l}^{l} dx A_B E(x)\frac{d\Omega}{4\pi}\quad , \tag{A2}$$

where

$$d\Omega=\frac{A_D\cos\theta}{x^2+r^2}=\frac{rA_D}{(x^2+r^2)^{3/2}}\quad . \tag{A3}$$

Thus,

$$F_D=A_B A_D\frac{r}{4\pi}\int_{-l}^{l}\frac{E(x)dx}{(x^2+r^2)^{3/2}}\quad . \tag{A4}$$

When $E(x)=E=$ constant, then

$$F_D=A_B A_D\frac{Er}{4\pi}\frac{2l}{r^2\sqrt{l^2+r^2}}\quad . \tag{A5}$$

For $l\gg r$, i.e., an infinite beam, Eq. (A5) becomes

$$F_D=\frac{A_B A_D E}{2\pi r}\quad . \tag{A6}$$

Here the light flux only falls off by the reciprocal of the distance.

For $l\ll r$, i.e., a small source, Eq. (A5) becomes

$$F_D=A_D E\frac{A_B 2l}{4\pi r^2}=V_{obs}E\frac{A_D}{4\pi r^2} \tag{A7}$$

and the light flux falls off by the reciprocal of the square of the distance.

For $l\sim r$, i.e., a beam of finite length, Eq. (A5) becomes

$$F_D=A_B 2lE\frac{A_D}{4\pi r\sqrt{l^2+r^2}}=V_{obs}E\frac{A_D}{4\pi r\sqrt{r^2+l^2}}\quad . \tag{A8}$$

Since $(l^2+r^2)^{1/2}\simeq r$ in this case, Eq. (A8) is approximated by Eq. (A7), i.e., the falloff is as r^{-2}.

Suppose, however, that E decreases exponentially, as in the case of the beam-gas chemiluminescence, i.e.,

$$E(x)=E_0\exp(-\sigma_{tot}Nx)\quad . \tag{A9}$$

Then,

$$F_D=\int_{-l}^{l} dx A_B E_0\exp(-\sigma_{tot}Nx)\frac{d\Omega}{4\pi} \tag{A10}$$

$$\simeq A_B E_0\frac{d\Omega}{4\pi}\frac{1}{\sigma_{tot}N}\left[\exp(\sigma_{tot}Nl)-\exp(-\sigma_{tot}Nl)\right]\quad . \tag{A11}$$

Since $\sigma_{tot}Nl$ is small, Eq. (A11) becomes

$$F_D=A_B 2lE_0\frac{A_D}{4\pi r^2}\quad . \tag{A12}$$

Comparing Eq. (A12) with (A7) we conclude that for small $\sigma_{tot}Nl$ they are identical and the exponential decay of the

beam introduces no additional correction to the flux measurement.

[1]D. J. Eckstrom, S. A. Edelstein, and S. W. Benson, J. Chem. Phys. 60, 2930 (1974).
[2]G. Black, M. Luria, D. J. Eckstrom, S. A. Edelstein, and S. W. Benson, J. Chem. Phys. 61, 4932 (1974).
[3]D. J. Eckstrom, S. A. Edelstein, D. L. Huestis, B. E. Perry, and S. W. Benson, J. Chem. Phys. 63, 3828 (1975).
[4]R. H. Obenauf, C. J. Hsu, and H. B. Palmer, J. Chem. Phys. 57, 5607 (1972); 58, 2674E (1973); 58, 4693 (1973).
[5]C. J. Hsu, W. D. Krugh, and H. B. Palmer, J. Chem. Phys. 60, 5118 (1974).
[6]C. R. Jones and H. P. Broida, J. Chem. Phys. 59, 6677 (1973); 60, 4369 (1974).
[7]Ch. Ottinger and R. N. Zare, Chem. Phys. Lett. 5, 243 (1970); C. D. Jonah, R. N. Zare, and Ch. Ottinger, J. Chem. Phys. 56, 263 (1972); J. L. Gole and R. N. Zare, J. Chem. Phys. 57, 5331 (1972); R. C. Oldenborg, J. L. Gole, and R. N. Zare, J. Chem. Phys. 60, 4032 (1974); R. C. Oldenborg, Ph.D. Thesis, Columbia University (1975).
[8]R. Stair, W. E. Schneider, and J. K. Jackson, Appl. Opt. 2, 1151 (1963). The standard lamp supplied by Optronic Laboratories is certified by W. E. Schneider.
[9]C. R. Dickson, Ph.D. Thesis, Columbia University (1976).
[10]G. Loriot and T. Moran, Rev. Sci. Instrum. 46, 140 (1975).
[11]H. B. Palmer (private communication, preliminary results, July, 1976).
[12]C. R. Dickson and R. N. Zare, Chem. Phys. 7, 361 (1975).
[13]A. Yokozeki and M. Menzinger, Chem. Phys. 14, 427 (1976).
[14]M. Menzinger (private communication).

SPECTROSCOPIC STUDY OF Pb + F_2 CHEMILUMINESCENCE

C. R. Dickson* and R. N. Zare†

Department of Chemistry, Columbia University

New York, New York 10027

ABSTRACT

The chemiluminescent intensity resulting from the reaction of Pb with F_2 is studied under beam-gas conditions at F_2 pressures of 10^{-4} torr and in the presence of argon at ~ 7 torr. A series of 133 red degraded bandheads belonging to the $A(\Omega=\frac{1}{2}) - X_1\ ^2\Pi_{\frac{1}{2}}$ system in the wavelenth region of 400-540 nm are observed in the chemiluminescent spectrum obtained in the presence of argon. Since 69 of these bandheads are new, a vibrational reanalysis of the PbF $A-X_1$ system is made. Two new band systems in the 670-800 nm wavelength region are believed to result from emission between higher PbF states. Under beam-gas conditions, the variation of the chemiluminescent intensity as a function of metal flux and oxidant pressure shows that PbF^* results from the bimolecular reaction $Pb + F_2 \rightarrow PbF^* + F$. Energetic considerations based on the mass spectrometric value of $D_0^0(PbF)$ and the short wavelength cutoff in the beam-gas chemiluminescent spectrum rule out the reaction $Pb(^3P_0) + F_2$ as responsible for populating the PbF A state but suggest instead that it is the reaction of a metastable lead atom $Pb(^3P_1)$ or $Pb(^3P_2)$ with F_2, most likely the former.

*Present address: Materials Research Center, Allied Chemical P.O. Box 1021R, Morristown, NJ 07960.

†Present address: Chemistry Department, Stanford University, Stanford, CA 94305.

I. INTRODUCTION

The diatomic molecule PbF has been the subject of numerous spectroscopic investigations using standard emission and absorption techniques. In 1936 Morgan reported a single system of double-headed bands lying between 410 to 530 nm obtained by absorption in PbF_2 vapor heated to 1500 °C (1). Rochester made one of the earliest and most extensive studies by heating PbF_2 in a discharge (2). Six systems (A, B, C, D, E, and F) were found in emission, a subsystem B_2 was found in absorption, and a continuum was found in both emission and absorption. Since then, numerous investigators have increased the spectroscopic information on the PbF molecule (3-9). However, no known spectroscopic investigation of PbF by chemiluminescence techniques has been made. Since these studies often lead to new and unexpected results, the chemiluminescent spectra produced by the reaction of Pb with F_2 is presented here.

New spectroscopic information was found when the reaction occurred in the presence of argon at pressures of a few torr. The number of new bandheads for the $A(\Omega=\frac{1}{2}) - X_1\ ^2\Pi_{\frac{1}{2}}$ system in the chemiluminescent spectrum exceeds twice the number previously reported. Consequently, a reanalysis of the $A-X_1$ system improved

the determination of the vibrational constants over other studies (1,2). In the wavelength region between 670-800 nm, two new band systems are observed which appear to have not been seen previously. These band systems are attributed to the emission between new upper states of the PbF molecule.

Chemiluminescent spectra of PbF are also obtained in a beam-gas arrangement at fluorine pressures between 10^{-6} to 10^{-4} torr (single-collision conditions). Chemiluminescence studies under single-collision conditions not only provide spectroscopic information, but also an understanding of the dynamics of highly exothermic chemical reactions. Kinetic studies are made by monitoring the chemiluminescent intensity as a function of oxidant pressure and metal beam flux. These studies show that the reaction is bimolecular and the resulting chemiluminescent spectra are due to emission from PbF^*. The population distribution of the electronic and vibrational internal states of PbF produced by the reaction of Pb and F_2 are also presented. From energetic considerations evidence is presented showing that the reaction responsible for causing the chemiluminescence under single-collision conditions does not involve the ground state of lead $Pb(^3P_0)$ but rather one of the metastable states $Pb(^3P_1)$ or $Pb(^3P_2)$, most probably the former.

II. EXPERIMENTAL

The beam apparatus, LABSTAR, has been previously described (10,11). The apparatus includes a water-cooled Astro-oven (Astro-Industries, Inc.) that resistively heats a cylindrical graphite tube containing a cylindrical graphite crucible with an aperture of 0.1 cm in diameter. The entire crucible-heater arrangement is surrounded by three concentric tantalum heat shields. The crucible temperature is measured with a W 5% Re/W 26% Re thermocouple. The output is fed into an Electromax C.A.T. controller (Leeds and Northrup) that regulates the heater current with two silicon-controlled rectifiers alternately firing at 60 Hz. The lead metal (99.999% purity obtained from Alfa-Ventron Corp.) is placed inside the graphite crucible where it is heated until the pressure reaches 0.01-0.1 torr. At this vapor pressure the beam flux in the reaction zone is estimated to be 10^{16} atoms-cm^{-1}-sec^{-1}. The effusive lead beam enters the scattering chamber where the Pb reacts with F_2 to produce chemiluminescence. The F_2 (98% purity obtained from Matheson Corp.) is passed over anhydrous NaF to remove any HF that may be present. A ballast tank filled with these oxidants is used to maintain a constant pressure as the gas is bled into the reaction chamber through a micrometer needle valve. No provision is

made to collimate the F_2 gas beam and it fills essentially the entire reaction chamber. Since the fluorine is extremely reactive, the pressure readings may be in error by as much as a factor of two.

The chemiluminescence is detected with a 1 meter Interactive Technology Czerny-Turner spectrometer operated in first order with a Bausch and Lomb 1200 groove/mm grating blazed at 500 nm. A cooled photomultiplier (RCA C31034, gallium arsenide 128 photocathode) is attached to the exit slits of the spectrometer. The entire optical detection system is calibrated using an Optronic Laboratories Model 245C standard lamp to provide relative photon yields. An approximate absolute photon yield for the $Pb + F_2$ reaction is made by comparison to the photon yield of the $Sm + N_2O$ reaction (12).

The beam-gas apparatus has been modified to permit chemiluminescent reactions to be studied in the presence of a buffer gas, such as argon, at pressures of a few torr. The entire flow arrangement is shown in Fig. 1. Argon enters the Astro-oven chamber through a bottom port and passes by an open crucible containing the lead metal. The crucible is resistively heated by a graphite heater which is surrounded by a Zircar heat shield (a porous zirconia material obtained from Union Carbide). As the

argon flows past the crucible, it carries the lead metal into the upper chamber through a graphite chimney. The fluorine enters through a small diameter (< 1 mm) copper tube. The argon flow rate is adjusted until the chemiluminescent flame reaches the desired brightness. For the Pb + F_2 reaction the pressure of argon in the upper chamber is ≈ 7 torr.

III. CHEMILUMINESCENT SPECTRA

The beam-gas reaction of Pb with F_2 produces a diffuse, blue chemiluminescence that may indicate a long lifetime for the excited-state PbF molecules. A rapid scan at 50 nm/min of the low resolution (0.5 nm) chemiluminescent spectrum is shown in Fig. 2. The emission from the $A(\Omega=\frac{1}{2}) - X_1\ ^2\Pi_{\frac{1}{2}}$ is the prominent feature seen in the wavelength region 385-510 nm. A sharp rise at 406.9 nm is the (8,2) bandhead of the $A-X_1$ system. This bandhead is the short wavelength cutoff which places a lower bound on the dissociation energy of PbF (see section IV.C.). At shorter wavelengths a continuum is observed until the emission ceases at ~ 385 nm. No evidence of the $A(\Omega=\frac{1}{2}) - X_2\ ^2\Pi_{\frac{1}{2}}$ emission could be found in the beam-gas chemiluminescent spectrum.

A rapid scan at 50 nm/min of the low resolution (0.5 nm) chemiluminescent spectrum obtained from the reaction of Pb with F_2 in the presence of argon at ~ 7 torr is shown in Fig. 3. A continuum is evident in the 295-400 nm region followed by the dominant $A(\Omega=\frac{1}{2}) - X_1\ ^2\Pi_{\frac{1}{2}}$ emission from 400-550 nm. Initially, the smaller peaks in the 670-800 nm region were believed to be emission from the $A-X_2$ system. However, a slower scan at 2.5 nm/min and 0.1 nm resolution showed two distinct band systems, each composed

of four sequences (see Fig. 4). None of these bandheads were observed in the beam-gas chemiluminescent spectrum.

A total of 133 red-degraded bandheads were measured for the A-X_1 system and are listed in Table I. The total number of bandheads in the combined results of Morgan (1) and Rochester (2) is 64. All of these bandheads were also observed in the present study. The remaining 76 bandheads were assigned vibrational quantum numbers by fitting them into a Deslandres table. Assuming that the head is close to the band origin, the positions of the bandheads are given by

$$\nu = T_e + \omega_e'(v'+\tfrac{1}{2}) - \omega_e x_e'(v'+\tfrac{1}{2})^2 + \omega_e y_e'(v'+\tfrac{1}{2})^3 - \omega_e''(v''+\tfrac{1}{2}) + \omega_e x_e''(v''+\tfrac{1}{2})^2 - \omega_e y_e''(v''+\tfrac{1}{2})^3 \quad (1)$$

where the symbols have their traditional meanings. The PbF bandhead positions are fit to Eq. (1) by a least-squares computer program, and the results are given in Table II. The errors given in Table II represent one standard deviation. The large number of bandheads considerably improves the uncertainties in the vibrational constants over those obtained by Morgan and Rochester. Many of the measured bandhead positions agree to the calculated

positions within 1 or 2 cm^{-1} (see Table I).

Alternatively, a linear least squares fit can be performed (13) by forcing ω_e'' and $\omega_e x_e''$ to be the same for both subbands by allowing the spin-orbit constant A_v to vary linearly with $(v+\tfrac{1}{2})$, i.e.,

$$A_v = A_e + a_e(v+\tfrac{1}{2}) \ . \quad (2)$$

The spectroscopic constants found in this manner are listed in Table III. Since no emission from the $A(\Omega=\tfrac{1}{2})$ - $X_2\ ^2\Pi_{\frac{1}{2}}$ system was observed in the chemiluminescent spectra, the four bandheads listed by Barrow (14) were used in this analysis. The sparcity of data for the A-X_2 system is reflected in the uncertainty of A_e(10 cm^{-1}). The measured bandhead positions of the A-X_1 system can be recovered from the following expression

$$\nu = T + \omega_e'(v'+\tfrac{1}{2}) - \omega_e x_e'(v'+\tfrac{1}{2})^2 + \tfrac{1}{2}A_v - \omega_e''(v+\tfrac{1}{2}) + \omega_e x_e''(v+\tfrac{1}{2})^2 . \quad (3)$$

The precise meaning of T is illustrated in Fig. 5 and should not be confused with T_e or T_{00}. Similarly, the bandhead positions for the A-X_2 state can be recovered by using Eq. (3), but by replacing $+\tfrac{1}{2}A_v$ with $-\tfrac{1}{2}A_v$. The uncertainties obtained by this fit are superior to that determined by the fit to Eq. (1).

The two band systems in the wavelength region 670-800 nm (see Tables IV and V) are arranged in a Deslandres scheme shown in Figs. 6 and 7. Only a relative vibrational numbering is possible because the emission does not terminate on a known PbF state. Since Barrow (3) has observed SiF band systems in emission that result from transitions between upper states, we believe these two PbF band systems also originate from transition between upper electronic states. A least-squares fit to the bandhead positions for the two band systems is made using Eq. (1). Table VI lists the approximate vibrational constants for these two band systems. No errors are given because the vibrational numbering is only relative and a good error analysis cannot be expected from a few bandheads.

It is interesting to note that we do not observe any emission from the A - X_2 $^2\Pi_{\frac{1}{2}}$ system. Our inability to observe this system may be due in part to the relatively strong emission from the new PbF systems which occur in the same wavelength region as the A-X_2 system. However, PbF is a heavy molecule and Hund's case c may be more applicable. Here, the $^2\Pi_{\frac{1}{2}}$ and $^2\Pi_{\frac{3}{2}}$ would become $(\frac{1}{2})$ and $(\frac{3}{2})$ states respectively in the case (c) coupling scheme. Perhaps it is not unreasonable to find that the $\frac{1}{2}$-$\frac{1}{2}$ and $\frac{1}{2}$-$\frac{3}{2}$ band systems have quite different intensities in emission.

IV. REACTION DYNAMICS

A. Internal State Distribution

In the beam-gas arrangement the pressure is so low that it is unlikely for the excited state product to experience a collision before it radiates. Consequently, the chemiluminescent spectrum should reflect the initial internal state distribution of PbF^* molecules formed in the reaction.

Within the PbF A-X band system, the relative vibrational distribution is determined from the intensity of emission for a particular bandhead. The intensity is obtained from the peak height of a band with the estimated contribution of neighboring bands subtracted out. The intensity must also be corrected for detector response in the wavelength region of interest. The $\Delta v = -2$ and $\Delta v = -3$ sequences are chosen because they show the least overlap with other bandheads. The intensities (photons/sec) are divided by $q_{v'v''}\nu^3(v',v'')$, the product of the Franck-Condon factor and the cube of the emission frequency, to obtain the relative population of a particular v' level. The Franck-Condon factors are calculated using RKR potentials with Hulbert-Hirschfelder extensions. The vibrational constants for the A and X states are taken from this work, while the rotational

constants are taken from Singh et al. (8). Figure 8 shows the vibrational distribution $N_{v'}$ vs v'. The $N_{v'}$ obtained from the two sequences agree to within ~ 20%. The close agreement lends credence to the result, i.e., the vibrational population in the PbF A state is distinctly non-Boltzmann in character and peaks at v'=5. This suggests that the reaction responsible for the production of PbF^* does not proceed through a long-lived collision complex.

At higher pressures, the chemiluminescent intensity reaches a maximum which reflects the attenuation of the metal beam by the oxidant. From this maximum (12), the total phenomenological cross section for metal atom removal is estimated to be ~ 140 Å². A factor of two error is possible in the pressure measurement, making this value uncertain by a factor of 2. Using this cross section as an upper bound to the total reactive cross section, the absolute photon yield for this reaction is estimated to be 0.2%. This indicates that nearly all of the PbF reaction products are formed in the ground electronic state.

B. Reaction Order

The reaction order with respect to F_2 is determined by fitting the chemiluminescent intensity as a function of F_2 pressure, p, to the expression $p^n \exp(-\alpha p)$, where n is the reaction order and α is an attenuation factor. At low F_2 pressures ($< 10^{-4}$), the chemiluminescent intensity is a linear function of the F_2 pressure. This demonstrates that the reaction is first order in fluorine.

The reaction order with respect to Pb is determined by studying the chemiluminescent intensity as a function of oven temperature. When a plot of the logarithm of the intensity vs the reciprocal oven temperature ($°K^{-1}$) is made, the data fit a straight line whose slope corresponds to a heat of vaporization of 40 kcal/mole. This value is in fair agreement with the accepted value (15) of $\Delta H_{vap}(Pb)$ = 43.9±0.3 kcal/mole at 1100 °K. We conclude that the chemiluminescence is first order in Pb atoms.

It is tempting to think that the above allows us to demonstrate that this is Pb in its lowest level, i.e. $Pb(^3P_0)$. However, despite the fact that the metastable levels $Pb(^3P_1)$ and $Pb(^3P_2)$ lie 20.36 kcal/mole and 30.45 kcal/mole higher in energy, we cannot exclude them because our previous study (16) of the

Pb + O_3 chemiluminescent reaction indicated that metastable lead atoms are present to a small extent in our metal beam, presumably caused by a weak discharge. Moreover, subsequent studies have shown that under these conditions the metastable concentration scales with the vapor pressure (17). We thus write the bimolecular reaction responsible for producing the PbF A state as

$$Pb(^3P_{0,1,2}) + F_2(^1\Sigma_g^+) \rightarrow PbF^*(\Omega=\tfrac{1}{2}) + F(^2P_{\frac{1}{2},\frac{3}{2}}) \quad . \qquad (4)$$

In the next section we show that we can rule out the participation of $Pb(^3P_0)$ in Eq. (4) on energetic grounds.

C. Reaction Energetics

It is possible to determine from the chemiluminescent spectrum under single-collision conditions a lower bound to the bond dissociation energy of the diatomic product (18). Applying energy balance to Eq. (4) and neglecting the final relative translational energy of the products, the inequality

$$D_0^\circ(PbF) \geq D_0^\circ(F_2) + E_{int}(PbF) - E_{int}(F_2) - E_{int}(Pb) - E_{trans}^i \qquad (5)$$

provides a lower bound to $D_0^\circ(PbF)$. The average internal energies of F_2, Pb, and PbF, denoted by $E_{int}(F_2)$, $E_{int}(Pb)$, and $E_{int}(PbF)$, are measured from their lowest energy levels. The initial relative translational energy, E_{trans}^i, is measured in the center-of-mass frame. The dissociation energy of F_2 is taken to be 37.1 ± 1.2 kcal/mole (19).

The internal energy of F_2 includes both rotational and vibrational contributions. The rotational contribution is simply RT = 209 cm^{-1}. The vibrational contribution may be estimated by taking the average vibrational energy. However, to preserve the inequality in Eq. (5) we assume that reaction with F_2 molecules only in the v=1 level causes the population of the highest excited level of the PbF A state. We estimate then $E_{int}(F_2)$ = 1100 cm^{-1} (3.15 kcal/mole).

The initial relative translational energy is estimated from the expression (20)

$$\bar{E} = \tfrac{1}{2}kT_{eff} \qquad (6)$$

where

$$T_{eff} = \frac{T(Pb)m(F_2) + T(F_2)m(Pb)}{m(F_2) + m(Pb)} \quad . \qquad (7)$$

Here $T(Pb) = 1713\ ^{\circ}K$, and $T(F_2) = 300^{\circ}K$ yielding $\bar{E} = 1.23$ kcal/mole. The initial relative translational energy distribution for the $Pb + F_2$ reaction is expected to have a broad distribution (20). This large spread is the main source of error in determining a lower bound to $D_0^{\circ}(PbF)$. Over 13% of the collisions taking place during the $Pb + F_2$ reaction have more energy than $2\bar{E}$. Since collisions with large E_{trans}^{i} may be the mechanism for populating the highest PbF internal states, we take the initial translational energy to be $E_{trans}^{i} = 1.23 \pm 1.23$ kcal/mole (i.e. $\bar{E} \pm \bar{E}$).

The internal energy of PbF is found from the short wavelength cutoff of the chemiluminescent spectrum, the (8,2) bandhead of the $A\text{-}X_1$ system. The internal energy of PbF can then be found from either of the following expressions

$$E_{int}(PbF) = T_{00} + G'(8) - G'(0) \qquad (8)$$

or

$$E_{int}(PbF) = E_{SWCO} + G''(2) - G''(0) \ . \qquad (9)$$

Here $G(v)$ and T_{00} have their traditional meanings and E_{SWCO} is the energy corresponding to the short wavelength cutoff. The

spectroscopic constants are those listed in Table II. Using these values in Eq. (8) and Eq. (9), $E_{int}(PbF)$ is 25 567.2 cm^{-1} and 25 566.7 cm^{-1}, respectively. Each of these values correspond to $E_{int}(PbF) = 73.10$ kcal/mole. Upon substitution into Eq. (5) we obtain

$$D_0^{\circ}(PbF) \geq 105.8 \pm 2 \text{ kcal/mole} - E_{int}(Pb) \ . \qquad (10)$$

This leads us to three possibilities, depending on which fine structure component of the ground state lead atom is responsible for causing the observed PbF^* emission:

$$D_0^{\circ}(PbF) \geq 105.8 \pm 2 \text{ kcal/mole} \qquad Pb(^3P_0) + F_2 \ , \qquad (11)$$

$$D_0^{\circ}(PbF) \geq 83.4 \pm 2 \text{ kcal/mole} \qquad Pb(^3P_1) + F_2 \ , \qquad (12)$$

and

$$D_0^{\circ}(PbF) \geq 75.3 \pm 2 \text{ kcal/mole} \qquad Pb(^3P_2) + F_2 \ , \qquad (12)$$

Fortunately, the bond dissociation energy of PbF seems now to be well established as 85±2 kcal/mole, based on the mass spectrometric studies of Zmbov, Hastie, and Margrave (21).

It follows then that the reaction $Pb(^3P_0) + F_2$ has insufficient energy to produce the observed PbF^* A state, whereas reaction of F_2 with either $Pb(^3P_1)$ or $Pb(^3P_2)$ is permitted on solely energetic grounds. The close agreement between the lower bound to $D_0^0(PbF)$ given in Eq. (12) and the present best value suggests that it is the metastable lead atom $Pb(^3P_1)$, alone, that reacts with F_2 under our experimental conditions to cause the production of the PbF A state. We do not know the concentration ratio of $Pb(^3P_1)$ to $Pb(^3P_2)$ in our beam and therefore we are reluctant to speculate further about the reaction dynamics of $Pb(^3P_0)$ with F_2.

ACKNOWLEDGMENT

We are grateful for useful correspondence with R. F. Barrow, D. L. Hildenbrand, and G. M. Rosenblatt concerning the PbF bond energy. This work is supported by the Army Research Office under grant DAAG29-76-G-0208 and by the Advanced Research Projects Agency of the Department of Defense, monitored by the Office of Naval Research under contract N00014-76-C-0466.

REFERENCES

1. F. Morgan, Phys. Rev. 49, 47 (1936).
2. G. D. Rochester, Proc. Roy. Soc. A155, 173 (1938).
3. R. F. Barrow, D. Butler, J. W. C. Johns, and J. L. Powell, Proc. Phys. Soc. 73, 317 (1959).
4. K. M. Rao and P. T. Rao, Can. J. Phys. 42, 690 (1964).
5. Y. P. Reddy and P. T. Rao, Proc. Int. Conf. Spectr., Bombay 1, 129 (1967).
6. O. N. Singh and I. S. Singh, Proc. Int. Conf., Bombay 1, 333 (1967).
7. S. P. Singh, Ind. J. Pure Appl. Phys. 5, 292 (1967).
8. O. N. Singh, M. P. Srivastava, and I. S. Singh, Can. J. Phys. 47, 1639 (1969).
9. O. N. Singh, I. S. Singh, and O. N. Singh, Can. J. Phys. 50, 2206 (1972).
10. R. C. Oldenborg, J. L. Gole, and R. N. Zare, J. Chem. Phys. 60, 4032 (1974).
11. R. C. Oldenborg, Ph.D. Thesis, Columbia University, 1975.
12. C. R. Dickson and R. N. Zare, Chem. Phys. 7, 361 (1975); C. R. Dickson, S. M. George, and R. N. Zare, J. Chem. Phys. (accepted for publication).
13. H. W. Cruse, P. J. Dagdigian, and R. N. Zare, Faraday Disc. Chem. Soc. 55, 277 (1975).
14. B. Rosen, Selected Constants Spectroscopic Data Relative to Diatomic Molecules, Pergamon Press, New York, 1970.
15. R. Hultgren, P. D. Desai, D. T. Hawkins, M. Gleiser, K. K. Kelley, and D. D. Wagman, Selected Values of the Thermodynamic Properties of the Elements (American Society for Metals, Metals Park, Ohio, 1973).
16. R. C. Oldenborg, C. R. Dickson, and R. N. Zare, J. Mol. Spectrosc. 58, 283 (1975).
17. R. C. Estler and R. N. Zare (unpublished work).
18. J. L. Gole and R. N. Zare, J. Chem. Phys. 57, 5331 (1972); R. N. Zare, Ber. Bunsenges. physik Chem. 78, 153 (1974).
19. J. Blauer and W. Solomon, J. Chem. Phys. 57, 3587 (1972).
20. P. J. Dagdigian, H. W. Cruse, and R. N. Zare, J. Chem. Phys. 62, 1824 (1975).
21. K. Zmbov, J. W. Hastie, and J. L. Margrave, Trans. Faraday Soc. 64, 861 (1968).

FIGURE CAPTIONS

Fig. 1. Schematic view of apparatus used to generate chemiluminescent reactions at pressures of several torr argon.

Fig. 2. Chemiluminescent spectra for the beam-gas reaction of Pb with F_2 taken at 0.5 nm resolution and a scan rate of 50 nm/min.

Fig. 3. Chemiluminescent spectra for the reaction of Pb with F_2 in the presence of argon taken at 0.5 nm resolution and a scan rate of 50 nm/min.

Fig. 4. Portion of the chemiluminescent spectra in the wavelength region of 670-800 nm. The resolution is 0.1 nm and the scan rate is 5 nm/min. System 1 is on the right, while system 2 is on the left.

Fig. 5. The term separation T is measured between the minimum of the A $\Omega=\frac{1}{2}$ potential curve and a point equidistant from the minima of the X_1 and X_2 potentials of the $^2\Pi$ state.

Fig. 6. Deslandres scheme for new PbF state (system 1).

Fig. 7. Deslandres scheme for new PbF state (system 2).

Fig. 8. Plot of the relative population $N_{v'}$, as a function of v' in the A($\Omega=\frac{1}{2}$) state for the $Pb+F_2$ beam-gas reaction. The distribution is non-Boltzmann peaking at v'=5.

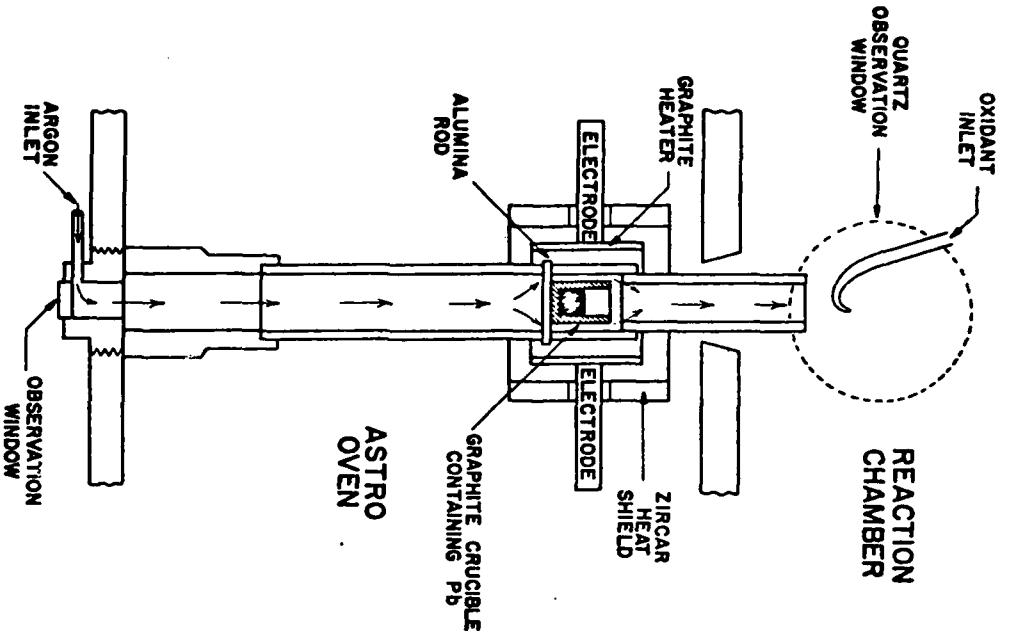

Fig. 1

$$Pb + F_2 \longrightarrow PbF^* + F$$

BEAM – GAS CHEMILUMINESCENCE

$$A(\Omega=1/2) \longrightarrow X_1\,^2\Pi_{1/2}$$

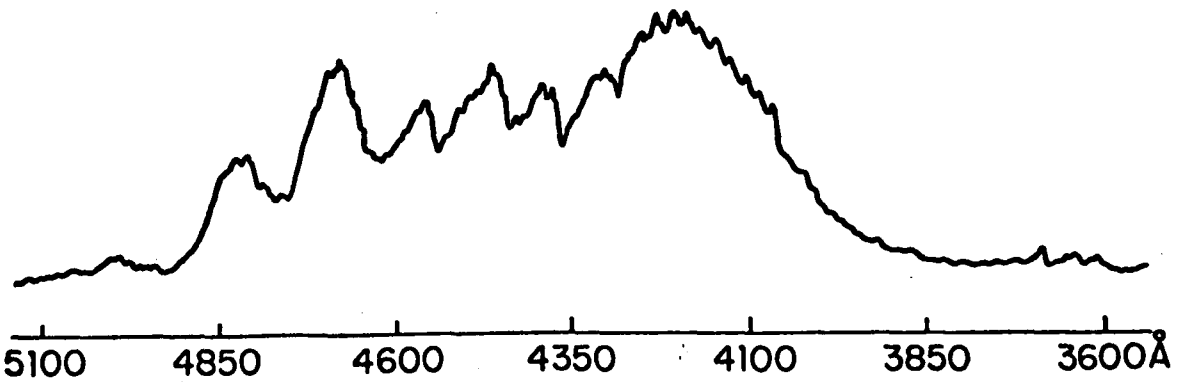

Fig. 2

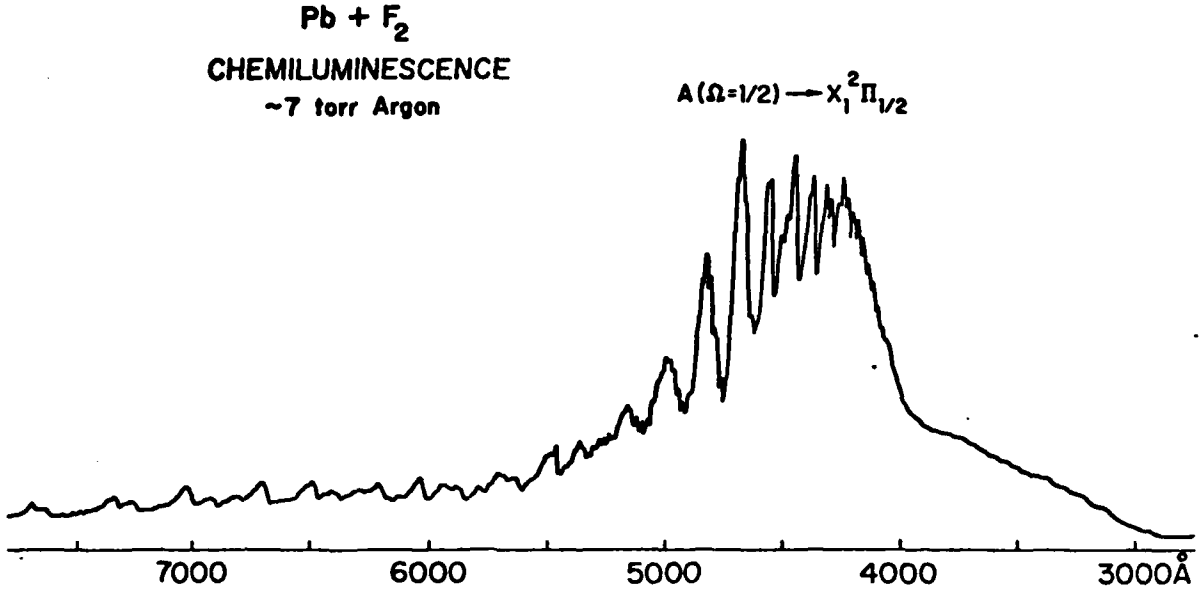
Pb + F2
CHEMILUMINESCENCE
~7 torr Argon
A(Ω=1/2) → X1 2Π1/2
7000
6000
5000
4000
3000Å

Fig. 3

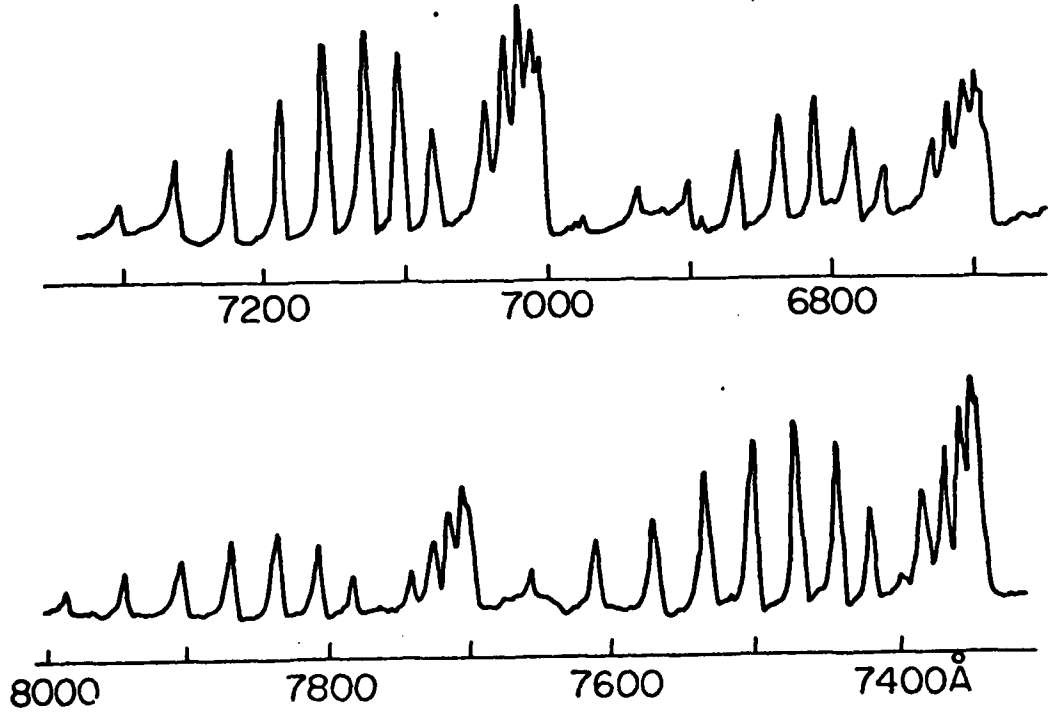
7200
7000
6800
8000
7800
7600
7400Å

Fig. 4

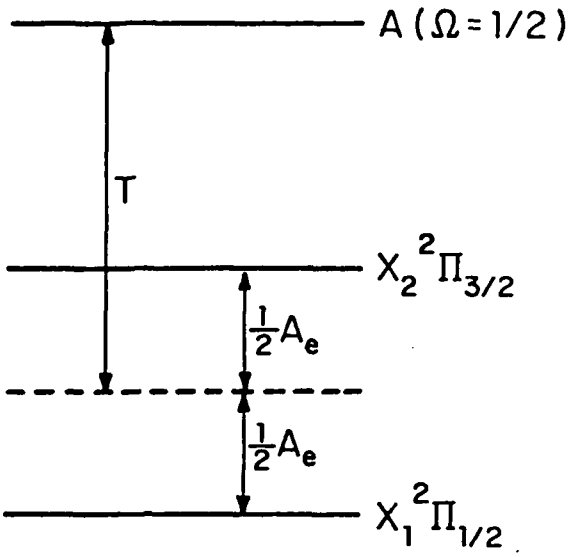

Fig. 5

v'' / v'	n	n+1	n+2	n+3	n+4	n+5	n+6	n+7	n+8	n+9
n	14964									
n+1	14921	14286								
n+2	14899	14255	13633							
n+3	14868	14233	13604	12992						
n+4	14824	14214	13583	12967						
n+5				13557	12948					
n+6					13524	12923				

Fig. 6

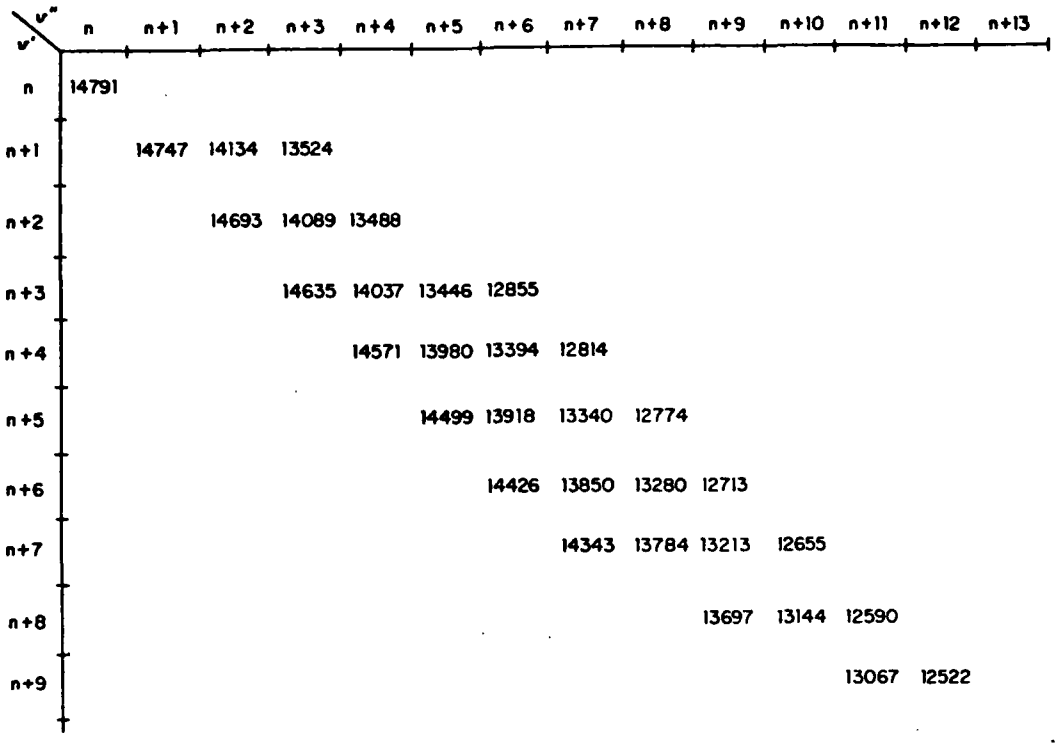
v''
v'
n
n+1
n+2
n+3
n+4
n+5
n+6
n+7
n+8
n+9
n+10
n+11
n+12
n+13
14791
14747 14134 13524
14693 14089 13488
14635 14037 13446 12855
14571 13980 13394 12814
14499 13918 13340 12774
14426 13850 13280 12713
14343 13784 13213 12655
13697 13144 12590
13067 12522

Fig. 7

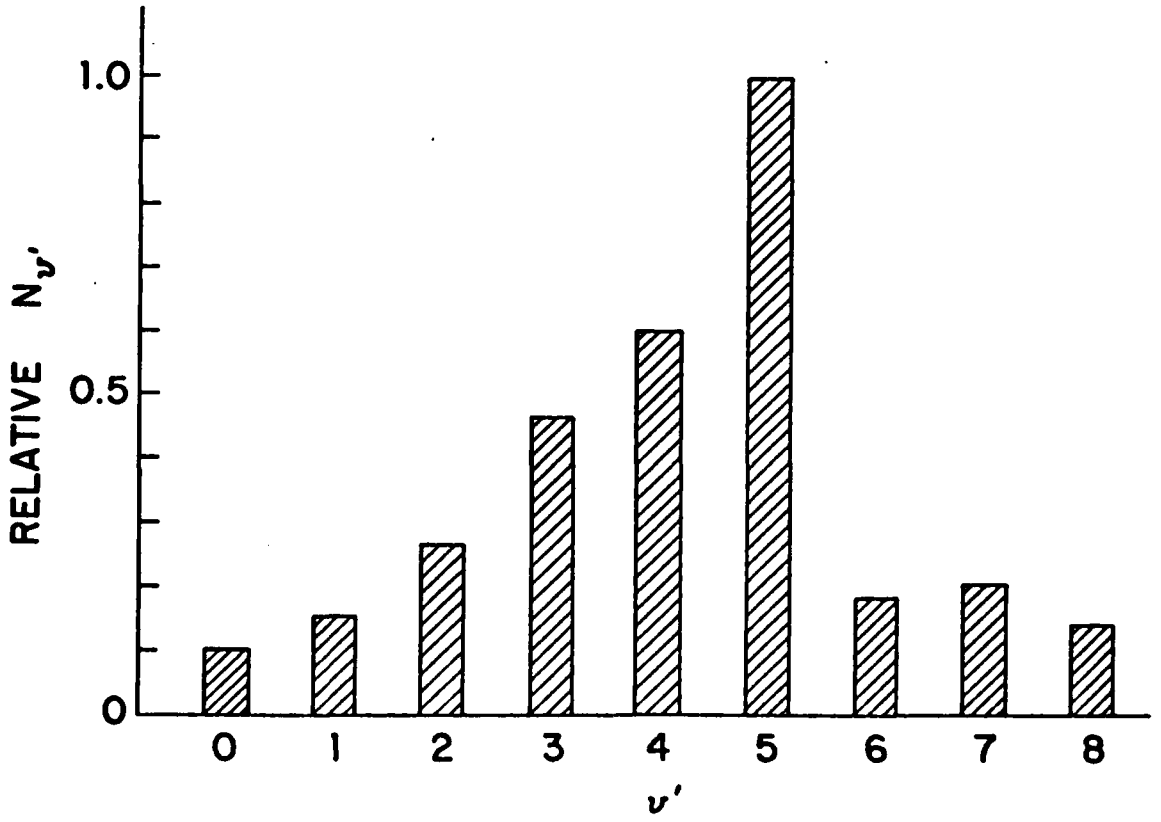
RELATIVE $N_{v'}$
1.0
0.5
0
0 1 2 3 4 5 6 7 8
v'

Fig.

TABLE I

Measured PbF Bandwidth Positions for $A(\Omega=1/2)-X_1^2\Pi_{1/2}$ Emission

bandhead assignment (v', v'')	bandhead position ν (cm^{-1})	$\nu_{obs.}-\nu_{calc.}$ (cm^{-1})	relative intensity	remarks
(9,2)	24932.5	-1.7	0	
(6,0)	24829.7	5.4	0	
(7,1)	24705.6	-9.8	2	
(8,2)	24567.3	-0.8	2	
(5,0)	24444.2	-3.2	3	
(6,1)	24321.5	-1.0	4	1
(7,2)	24199.7	1.3	4	1
(8,3)	24075.1	-0.1	3	1
(4,0)	24067.6	0.6	6	1
(9,4)	23951.7	-1.1	3	
(5,1)	23945.1	-0.6	6	1
(6,2)	23823.4	-1.8	6	1,2
(7,3)	23704.1	-1.4	5	
(3,0)	23680.7	-8.2	6	1,2
(8,4)	23585.5	-1.2	3	
(4,1)	23565.2	0.0	7	1
(5,2)	23448.3	0.0	5	1,2
(10,6)	23350.8	0.7	1	
(6,3)	23333.4	1.2	2	
(2,0)	23296.5	1.2	7	1,2
(7,4)	23215.3	-1.7	3	
(3,1)	23178.9	-2.3	6	1,2
(8,5)	23101.0	-1.6	3	
(4,2)	23067.2	-0.7	3	1,2
(9,6)	22991.0	2.0	3	1,2
(5,3)	22954.1	-1.3	8	
(1,0)	22905.1	1.0	9	1,2
(10,7)	22875.6	-0.4	0	
(6,4)	22644.5	0.8	0	
(2,1)	22794.6	1.1	4	1
(7,5)	22729.4	-3.5	3	1
(3,2)	22685.3	1.5	1	
(8,6)	22621.7	-1.2	2	
(4,3)	22573.1	-1.8	2	1
(0,0)	22509.6	0.3	10	1,2
(5,4)	22464.6	-2.3	7	1
(1,1)	22406.2	3.9	4	1
(6,5)	22365.1	5.5	3	
(2,2)	22296.2	0.0	4	1,2
(7,6)	22251.6	-1.6	4	
(3,3)	22190.3	-0.6	4	1,2
(8,7)	22149.5	1.9	3	
(4,4)	22084.0	-2.4	1	1,2
(0,1)	22008.6	1.1	10	1,2
(5,5)	21978.6	-4.1	0	
(1,2)	21905.3	0.3	4	1,2

TABLE I (cont'd)

bandhead assignment (v', v'')	bandhead position ν (cm^{-1})	$\nu_{obs.}-\nu_{calc}$ (cm^{-1})	relative intensity	remarks
(6,6)	21875.1	-0.8	0	
(7,7)	21777.5	-0.4	0	
(3,4)	21703.2	-1.7	0	1
(8,8)	21675.1	-1.7	1	1
(4,5)	21601.1	-1.2	2	1,2
(9,9)	21576.4	0.0	0	
(0,2)	21510.9	0.8	8	1,2
(10,10)	21476.3	-0.6	0	
(1,3)	21412.0	0.0	9	1,2
(11,11)	21382.6	4.4	0	
(2,4)	21314.1	-0.6	6	1,2
(7,8)	21308.7	1.6	0	
(3,5)	21216.5	-1.8	0	1,2
(8,9)	21214.2	3.9	0	
(4,6)	21124.6	2.0	0	
(5,7)	21024.6	-3.2	0	
(0,3)	21016.1	-1.1	3	1,2
(6,8)	20932.0	-1.8	0	2
(1,4)	20923.2	-0.3	6	1,2
(7,9)	20839.1	-1.5	0	2
(2,5)	20830.1	-0.5	7	1,2
(8,10)	20746.1	-2.2	0	2
(3,6)	20736.9	-1.7	7	1,2
(9,11)	20655.4	-1.4	0	1,2
(4,7)	20646.2	-1.1	4	1,2
(5,8)	20555.9	-1.0	2	1,2
(0,4)	20529.7	1.0	1	1,2
(1,5)	20441.3	1.9	2	1,2
(7,10)	20360.0	1.4	0	
(2,6)	20350.6	-0.3	3	1,2
(8,11)	20292.1	1.4	0	1
(3,7)	20262.7	-0.6	3	1,2
(9,12)	20204.1	0.5	1	
(4,8)	20176.7	0.2	4	1,2
(10,13)	20119.6	2.3	0	
(5,9)	20091.9	1.4	4	1,2
(0,5)	20043.9	-0.7	0	
(11,14)	20031.7	-0.1	0	
(6,10)	20005.2	-0.1	3	1,2
(1,6)	19959.9	0.2	2	1
(7,11)	19920.8	-0.2	1	1,2
(2,7)	19876.5	0.8	1	1,2
(8,12)	19836.9	-0.6	1	
(3,8)	19793.4	1.0	1	1,2
(9,13)	19753.8	-1.0	0	
(4,9)	19710.4	0.3	0	2

TABLE I (cont'd)

bandhead assignment (v', v'')	bandhead position ν (cm^{-1})	$\nu_{obs.} - \nu_{calc.}$ (cm^{-1})	relative intensity	remarks
(5,10)	19628.9	0.4	0	1,2
(0,6)	19559.6	-5.1	0	
(6,11)	19549.2	1.5	0	1,2
(1,7)	19483.6	-0.8	0	
(7,12)	19469.1	1.3	0	1,2
(2,8)	19402.3	-2.5	0	1,2
(8,13)	19389.2	0.5	0	1,2
(3,9)	19320.5	0.5	0	2
(4,10)	19246.7	0.7	0	
(10,15)	19231.7	-1.3	0	1,2
(5,11)	19172.3	1.4	0	
(11,16)	19156.2	-0.2	0	2
(6,12)	19095.6	1.1	0	1,2
(7,13)	19020.4	1.4	0	1
(8,14)	18946.3	1.9	0	
(9,15)	18870.2	-0.3	0	
(10,16)	18799.5	2.0	0	
(6,13)	18646.3	0.5	0	
(8,8)	18617.1	-1.7	0	
(7,14)	18575.3	0.6	0	
(1,9)	18547.0	-0.1	0	
(8,15)	18507.5	3.1	0	
(2,10)	18479.5	3.2	0	
(9,16)	18422.5	-2.5	0	
(10,17)	18368.5	2.1	0	
(4,12)	18339.2	2.0	0	
(11,18)	18297.5	-1.1	0	
(5,13)	18267.4	-1.5	0	
(6,14)	18197.6	-3.8	0	
(0,9)	18156.0	3.4	0	
(7,15)	18135.9	1.2	0	
(1,10)	18089.6	4.5	0	
(6,16)	18070.0	1.1	0	
(2,11)	18017.2	-1.5	0	
(9,17)	18001.3	-2.6	0	
(10,18)	17986.0	-1.7	0	
(9,13)	17892.1	3.6	0	
(11,19)	17872.9	-3.4	0	
(7,16)	17697.7	1.5	0	
(0,10)	17686.4	-3.9	0	
(2,12)	17565.8	0.3	0	

1 observed by Morgan (1).
2 observed by Rochester (2).

TABLE II

VIBRATIONAL CONSTANTS OF PbF
$A\,(\Omega=1/2) - X^2\Pi_{1/2}$ BAND SYSTEM

CONSTANT	VALUE FROM THIS WORK (cm^{-1})	VALUE FROM MORGAN (REF. 1) (cm^{-1})	VALUE FROM ROCHESTER (REF. 2) (cm^{-1})
T_e	22564.9 ± 8.0	22565.2	22567
ω_e'	398.443 ± 0.3	397.8	397.8
$\omega_e x_e'$	1.81958 ± 0.01	1.77	1.77
$\omega_e y_e'$	0.00233696 ± 0.00004		
ω_e''	507.288 ± 0.1	506.9	507.2
$\omega_e x_e''$	2.35844 ± 0.002	2.29	2.30
$\omega_e y_e''$	0.00553828 ± 0.000002		

TABLE III

VIBRATIONAL CONSTANTS OF PbF
$A(\Omega=1/2) - X^2\Pi$ BAND SYSTEM

VIBRATIONAL CONSTANT	VALUE (cm^{-1})
T	18428.4 ± 6.1
ω_e'	398.409 ± 0.565
$\omega_e x_e'$	1.79557 ± 0.004
ω_e''	519.445 ± 0.244
$\omega_e x_e''$	2.20795 ± 0.0007
A_e	8269.29 ± 10.05
α_e	26.5251 ± 0.9492

TABLE IV

Measured PbF Bandhead Positions for System 2 in the 670 to 800 nm Wavelength Region

sequence	bandhead position (cm^{-1})	$\nu_{obs.} - \nu_{calc.}$	sequence	bandhead position (cm^{-1})	$\nu_{obs.} - \nu_{calc.}$
$\Delta v = n$	14791.0	-1.8	$\Delta v = n-2$	13487.9	-0.1
	14747.4	1.1		13446.2	1.9
	14693.2	-0.5		13394.0	-0.8
	14635.1	-0.2		13213.4	0.5
	14571.1	-0.2		13340.3	0.7
	14499.3	-2.5		13260.1	1.2
	14343.2	-4.3		13066.6	0.6
	14426.0	-1.2			
$\Delta v = n-1$	14134.4	2.3	$\Delta v = n-3$	12654.9	-4.6
	14068.6	1.5		12613.7	3.5
	14037.1	0.9		12774.4	5.5
	13980.2	0.7		12712.7	-2.3
	13917.9	0.7		12589.4	-1.6
	13850.4	0.8		12521.6	-0.1
	13783.6	6.8			
	13696.7	-2.4			

TABLE V

Measured PbF Bandhead positions for System 1 in the 670 to 800 nm Wavelength Region

sequence	band head position (cm^{-1})	$\nu_{obs} - \nu_{calc}$ (cm^{-1})
$\Delta v = n$	14963.7	2.3
	14921.3	-5.2
	14899.0	4.3
	14868.0	4.5
	14823.9	-6.6
$\Delta v = n-1$	14285.9	1.2
	14255.3	-4.5
	14233.0	-0.3
	14214.0	8.8
$\Delta v = n-2$	13633.2	3.6
	13603.5	-4.5
	13583.2	-1.7
	13557.4	-0.7
	13524.4	-0.5
$\Delta v = n-3$	12991.9	4.1
	12966.6	-3.5
	12948.1	-0.7
	12923.0	1.6

TABLE VI

APPROXIMATE VIBRATIONAL CONSTANTS OF NEW PbF BAND SYSTEMS

VIBRATIONAL CONSTANT	VALUE FOR SYSTEM 1 (cm^{-1})	VALUE FOR SYSTEM 2 (cm^{-1})
ΔT_e	14980.7	14813.8
ω_e'	607.4	589.5
$\omega_e x_e'$	1.39	7.1
$\omega_e y_e'$	0.44	0.06
ω_e''	647.7	629.8
$\omega_e x_e''$	1.96	3.96
$\omega_e y_e''$	0.04	0.02